Impact of Data Assimilation on Ocean Initialization and El Niño Prediction

MING JI AND ANTS LEETMAA

National Centers for Environmental Prediction, National Weather Service/NOAA, Washington, D.C.

(Manuscript received 24 February 1995, in final form 12 July 1995)

ABSTRACT

In this study, the authors compare skills of forecasts of tropical Pacific sea surface temperatures from the National Centers for Environmental Prediction (NCEP) coupled general circulation model that were initiated using different sets of ocean initial conditions. These were produced with and without assimilation of observed subsurface upper-ocean temperature data from expendable bathythermographs (XBTs) and from the Tropical Ocean Global Atmosphere–Tropical Atmosphere Ocean (TOGA–TAO) buoys.

These experiments show that assimilation of observed subsurface temperature data in the determining of the initial conditions, especially for summer and fall starts, results in significantly improved forecasts for the NCEP coupled model. The assimilation compensates for errors in the forcing fields and inadequate physical parameterizations in the ocean model. Furthermore, additional skill improvements, over that provided by XBT assimilation, result from assimilation of subsurface temperature data collected by the TOGA–TAO buoys. This is a consequence of the current predominance of TAO data in the tropical Pacific in recent years.

Results suggest that in the presence of erroneous wind forcing and inadequate physical parameterizations in the ocean model ocean data assimilation can improve ocean initialization and thus can improve the skill of the forecasts. However, the need for assimilation can create imbalances between the mean states of the oceanic initial conditions and the coupled model. These imbalances and errors in the coupled model can be significant limiting factors to forecast skill, especially for forecasts initiated in the northern winter. These limiting factors cannot be avoided by using data assimilation and must be corrected by improving the models and the forcing fields.

1. Introduction

The most significant climate variability on the interannual timescale is related to the El Niño–Southern Oscillation (ENSO) phenomenon. El Niño–related climate anomalies in atmospheric height, temperature, and precipitation fields have been documented by many studies (Bjerknes 1969; Horel and Wallace 1981; Ropelewski and Halpert 1986,1987; Rasmusson and Wallace 1983). These climate anomalies often have global socioeconomic impacts. Hence, in addition to being an exciting, tractable scientific problem, forecasting of El Niño and the associated climate variability in the extratropics has important human impacts.

The coupled ocean–atmosphere model of Cane et al. (1986) was the first dynamical model that achieved success in forecasting warm and cold ENSO episodes. Subsequently, a number of dynamical coupled forecast models of various degrees of complexity have been developed and have demonstrated skill for forecasting El Niño and interannual variability of the coupled tropical ocean–global atmosphere system (Latif and Flügel 1991; Barnett et al. 1993; Latif et al. 1993, 1994; Ji et al. 1994; Kleeman et al. 1995).

Because of the greater heat capacity of the ocean compared to the atmosphere, the memory of the coupled climate system that allows predictability is believed to reside in the ocean (Wyrtki 1975, 1985). Therefore, accurate knowledge of ocean initial conditions is necessary for forecasting seasonal to interannual climate variability. Because tropical oceanic circulations are primarily driven by the surface wind stress, a straightforward initialization of the ocean is to force an ocean model with observed surface wind stresses up to the times when forecasts are initiated. Of the dynamical coupled forecast models mentioned above, most of them use this technique. The Florida State University (FSU) surface wind stress analysis (Goldenberg and O'Brien 1981) is the forcing field used by those models.

The coupled general circulation model (CGCM) of Ji et al. (1994) used an ocean-model-based data assimilation system (Derber and Rosati 1989; Ji et al. 1995) to achieve analyzed ocean fields as initial conditions for their coupled model. The ocean data assimilation system (ODAS) assimilates all available subsurface temperature data from expendable bathythermographs (XBTs) and the Tropical Ocean Global Atmosphere–Tropical Atmosphere Ocean (TOGA–TAO) moored

Corresponding author address: Dr. Ming Ji, Coupled Model Project, National Centers for Environmental Prediction, 5200 Auth Road, Room 807, Camp Springs, MD 20746.
E-mail: wd01mj@sgi12.wwb.noaa.gov

buoys (McPhaden 1993), as well as surface information from ships, buoys, and satellite, into the ocean model using the model temperature fields as the first guess. This coupled forecast model, as well as a similar forecast system developed by Rosati et al. (1997), shows significant skill for eastern equatorial Pacific sea surface temperature (SST) forecasts, which is comparable to or higher than persistence forecasts at lead times of one month and longer. In contrast, coupled forecast models in which the ocean is spun up using the FSU wind stresses without data assimilation and without using observed SST generally do not have skills that are higher than persistence forecasts at lead times of shorter than about four to five months (Latif et al. 1993; Neelin et al. 1994). Recently, Kleeman et al. (1995) used an adjoint method to assimilate the FSU winds and subsurface thermal information derived from an ocean analysis into an intermediate coupled model for ocean initialization. They also found that improved forecast skill is achieved over forecasts that were initialized using the FSU winds alone.

A major reason for using ODAS for initialization is that significant errors exist in both wind stress forcing fields and in ocean models. These errors are difficult to overcome at present, and therefore assimilation of observed in situ data is used to correct for these forcing and model errors. A recent study by Ji and Smith (1995) compared ocean model fields produced using the same wind stress forcing (FSU), that is, the one used in most forecast models but with and without assimilation of subsurface thermal data. Their results show that ocean analyses produced with data assimilation are of higher quality than those produced without data assimilation when compared to independent in situ observations of sea level records.

Despite these positive indications that initialization of the ocean utilizing subsurface data assimilation improves the forecast skill, the impact of ocean initialization using data assimilation on seasonal to interannual climate predictions needs further study. Although present data assimilation techniques provide compensation for errors in forcing and in ocean models, use of higher quality wind stress forcing fields still incrementally improves the ocean analyses (Ji and Smith 1995). However, initialization of all scales of ocean variability might not lead to increased forecast skill for El Niño because those of short timescale and small spatial-scale ocean variability are often not relevant to ENSO, a low frequency basin-scale phenomenon (Chen et al. 1995). At some point, other factors in existing coupled forecast systems—such as model errors, synoptic-scale noises in atmospheric forcing fields, imbalances between ocean initial conditions and the coupled forecast model that result in initial shocks, and the inherent predictability limits of the coupled system—will become the limiting factors in forecast skill. How close current assimilation procedures have brought us to this limit needs to be examined.

A decade-long international research program to understand and document interactions between the tropical ocean and global atmosphere on seasonal to interannual timescales and to study potential predictability of this component of climate variability was launched in 1985. The TOGA program formally ended at the end of 1994. One significant achievement of the TOGA was the deployment of the TAO array of moored buoys in the equatorial Pacific (Hayes et al. 1991; McPhaden 1993). Subsurface temperature data from the TAO buoys have been used for ENSO monitoring and are an important data source for producing real time and retrospective ocean analyses (Ji et al. 1995). The value of the TAO data in climate analysis and monitoring is well documented (Reynolds et al. 1989; McPhaden 1993; Halpern and Ji 1993; Ji et al. 1995). On the other hand, the value of the TAO data in seasonal to interannual climate prediction needs to be evaluated. This can be done by evaluation of forecasts initialized with and without surface wind and subsurface thermal data from the TAO array. The short data record precludes a definitive study; however, these preliminary results suggest a positive impact of the TAO data on forecast skill.

The primary objective of this study is to document the impact of subsurface thermal data assimilation on ocean initialization and El Niño prediction by comparing forecasts initiated using ocean initial conditions produced with and without assimilating subsurface thermal data and to present our first experiments using the TOGA–TAO moored buoy temperature data in the initialization of coupled climate forecasts. These will be presented in sections 4 and 5. A brief description of the models and the ocean analysis system is given in section 2; various ocean initial conditions and the corresponding coupled model forecasts are discussed in section 3. A summary is provided in section 6.

2. A description of the models and the ocean analysis system

The ocean general circulation model (OGCM) was developed at Geophysical Fluid Dynamics Laboratory (GFDL) by Bryan (1969) and Cox (1984) and subsequently improved by Philander et al. (1987). The National Centers for Environmental Prediction (NCEP, formerly the National Meteorological Center) version of the model is configured to cover the Pacific basin from 120°E to 70°W and from 45°S to 55°N. This model has 28 vertical levels. Its zonal resolution is 1.5°, and its meridional resolution is 1/3° in the equatorial Pacific within 10° of the equator. The meridional resolution reduces gradually to 1° poleward of 20° latitude. The same OGCM is used in the coupled model as in the ocean analysis system.

The atmospheric general circulation model (AGCM) used in the NCEP coupled model is a modified version of the NCEP's operational global medium-range forecast (MRF) model with a spectral resolution of T40 and

18 vertical levels. Modification to the physical parameterizations of the MRF resulted in significantly improved midlatitude response to tropical SST forcing, stronger surface stress, and better organized tropical precipitation patterns (Ji et al. 1994; Kumar et al. 1996).

The NCEP's coupled general circulation model (CGCM), which consists of these components, is described in Ji et al. (1994). It uses anomaly coupling for surface stress and shortwave flux, and full coupling for sensible, latent, and longwave heat fluxes. The choice for using anomalous coupling was to achieve a more realistic annual cycle and to reduce the climate drift of the coupled model because the stress and shortwave flux annual cycles produced from the AGCM simulation experiments exhibited large errors. The climatological annual cycle of wind stress of Hellerman and Rosenstein (1983) was used as the mean stress forcing field for the ocean; the annual cycle of climatological shortwave flux was estimated using the bulk formula of Reed (1977) and the mean annual cycle of cloudiness from the International Satellite Cloud Climatology Project (ISCCP). Stress and shortwave flux anomalies from the AGCM are obtained by removing the T40 MRF's climatologies. The AGCM's annual cycles were estimated from ensemble simulations using the T40 MRF alone forced with observed monthly mean SSTs for 1982–93 (Reynolds and Marsico 1993). In the remainder of this paper, this coupled model will be referred to as CMP6. Current operational forecast of tropical Pacific SSTs at NCEP are produced by a later version of this model which uses different ocean–atmosphere coupling. This system will be discussed in a future publication.

The ocean analysis system consists of the GFDL ocean model and a data assimilation system based on a four-dimensional variational objective analysis method (Derber and Rosati 1989). Observed surface and subsurface temperature data are assimilated into the ocean model continuously using the model's temperature field as the first guess. Monthly mean ocean analyses were produced retrospectively for 1982–94 for diagnostics of seasonal to interannual climate variability and for initialization and verification of CGCM forecasts (Ji et al. 1995). The ocean fields on the first day of every month were saved to be used as the initial conditions for forecast experiments.

3. Ocean initial conditions and forecast experiments

As indicated in the introduction, the primary objective of this study was to evaluate the impact of ocean data assimilation on multiseason tropical Pacific SST predictions using CGCMs. For this purpose, several sets of ocean initial conditions were produced using different wind stress products with and without data assimilation. Each set was used to initiate a set of forecasts. In this section, we will describe these ocean initial conditions and the corresponding forecast experiments. Evaluation of the forecasts and intercomparisons will be presented in subsequent sections.

The first initial condition dataset, denoted as RA2, was produced using the ocean analysis system for the period of 1982–93. All available surface and subsurface temperature data were used in the assimilation. This dataset was described in Ji et al. (1995). The OGCM was forced with a hybrid stress forcing field that consists of a mean annual cycle stress climatology (Harrison 1989), in which the amplitude was increased by a factor of 1.1, and an anomalous stress forcing. The anomalous stress forcing was obtained from the average of two 12-yr AGCM simulations forced with observed monthly SST. The corresponding forecast experiments, denoted as F-RA2 and using the CMP6 model, were carried out starting on the first of each month from October 1983 to October 1993. All the forecasts were 12 months in length.

The second dataset used for initialization, denoted as HFSU, was produced from an 11-yr ocean simulation. The OGCM was forced with climatological heat flux (Oberhuber 1988) and a hybrid stress forcing field that consists of the Hellerman and Rosenstein (1983) stress climatology and the monthly FSU stress anomalies for 1982–93. A set of 101 1-yr forecasts, denoted as F-HFSU, using the CMP6 model were carried out starting on the first of each month for January, February, and May through December, and for the period of October 1983 to October 1993. The F-HFSU forecast experiment is similar to those described by Latif et al. (1993) and Cane et al. (1986) in the sense that only wind information from the FSU analysis is provided to precondition the ocean for forecasts. Details of the RA2 and HFSU datasets are also described and evaluated in Ji and Smith (1995).

To examine the impact of the TOGA–TAO buoy data on forecast skill, a set of ocean initial conditions, denoted as NTAO, were produced using the ocean analysis system without assimilating subsurface temperature data from the TOGA–TAO buoys. Only subsurface temperature data from XBTs were assimilated. The wind stress forcing used for NTAO is the same as that used for the HFSU. A set of corresponding forecasts, denoted as F-NTAO, was carried out starting on the first of May through October for 1989–93 using the CMP6 model. The impact of subsurface thermal data assimilation on forecast skill can be evaluated through comparisons of the F-RA2, F-HFSU, and F-NTAO forecasts. These comparisons are presented in the next two sections.

The ocean initial conditions described above are summarized in Table 1. The corresponding forecast experiments are summarized in Table 2.

4. The impact of subsurface data assimilation

The time histories of the anomalous depth of the 20°C isotherm along the equator in the Pacific from 1982 to 1993 for RA2 and HFSU are shown in Fig. 1. The 20°C

TABLE 1. List of ocean initial conditions.

Name	Wind forcing	Obs. temp. data	Duration	Forecast exp.
RA2	1.1HCL + AMIP	All	July 1982–December 1993	F-RA2
HFSU	0.9H&R + FSUA	None	July 1982–December 1993	F-HFSU
NTAO	0.9H&R + FSUA	No TAO	May 1989–October 1993	F-NTAO

1.1 HCL:	Harrison (1989) stress climatology, amplitude increased by 1.1
AMIP:	Stress anomalies produced from 12-yr AGCM simulation forced with observed monthly SST.
0.9H&R:	Hellerman and Rosenstein (1983) stress climatology reduced by 0.9.
FSUA:	Stress anomalies produced from the FSU analyses.
ALL:	All available surface and subsurface temperature data were assimilated.
NONE:	No subsurface temperature data were assimilated.
NO TAO:	Observed subsurface temperature data from the TOGA–TAO buoys were not assimilated.

isotherm lies in the middle of the thermocline and variations in its depth are often used as a surrogate for thermocline and upper ocean heat content variations. In the eastern equatorial Pacific eastward of 150°W, the interannual variations of the thermocline are well captured by both RA2 and HFSU. The most significant features during the 1982–93 period are the warm episodes of 1982–83, 1986–87, and 1991–92, when positive depth anomalies were found in the eastern Pacific, and the two cold episodes of 1984–85 and 1988–89, when negative depth anomalies were observed in this region. In the western equatorial Pacific, west of 150°W, the HFSU exhibits significantly weaker variability as compared to the RA2. Comparisons to independent in situ observations from moorings and tide gauges (not shown) indicate that RA2 is closer to the observations than is the HFSU (Ji et al. 1995; Ji and Smith 1995).

A recent study by Hao and Ghil (1994) demonstrated that signals placed in the western equatorial Pacific result in a much stronger and faster basinwide tropical oceanic response than those placed in the eastern part of the basin. In the former case, signals travel eastward along the equator at fast Kelvin wave phase speeds. In contrast, signals placed in the eastern equatorial Pacific travel westward off the equator at a slower Rossby wave speed. They also often weaken significantly or even become completely lost before reaching the western boundary. This results in a weaker and slower ocean adjustment. Hao and Ghil (1994) concluded that initialization of the western and central equatorial Pacific may be more important than initialization of the eastern equatorial Pacific. This also seems to be true based on results from experiments using the Cane and Zebiak model (Zebiak and Cane 1989) and an improved ocean initialization procedure (Chen et al. 1995). The comparison in Fig. 1 suggests that it is in the western equatorial Pacific where subsurface temperature data assimilation plays a strong role in compensating for wind and model errors. Viewed from the perspective of the previous discussion, Fig. 1 implies that assimilation of subsurface temperature data should have a significant impact on forecast results.

TABLE 2. List of forecast experiments.

Name	Ocean init. cond.	Exp. period	Forecast length (months)
F-RA2	RA2	1 Oct 1983–1 Oct 1993	12
F-HFSU	HFSU	1 Oct 1983–1 Oct 1993*	12
F-NTAO	NTAO	1 May–1 Oct 1989–93	12

* F-HFSU forecasts were initiated on the first of January, February, and May–December for the period shown.

The two leading EOFs for the monthly mean difference fields of the depth of 20°C isotherm (H_{20} hereafter) between RA2 and HFSU (HFSU–RA2) are shown in Fig. 2. The time evolution of these two leading EOFs are shown in the lower panel of Fig. 2. The 12-yr (1982–93) average of the monthly H_{20} difference is removed prior to construction of the EOFs. This 12-yr mean difference field (not shown) has significant amplitude in the off-equatorial regions (Ji and Smith 1995). It reflects errors in the climatological mean state of the ocean resulting from errors in the mean climatological stress forcing and in the OGCM. This mean difference is thought to be responsible for the climate drift in the coupled forecast model and results in systematic errors in the forecast SST and thermocline depth fields (Mo et al. 1994).

In the equatorial region, the first EOF of the difference field exhibits an east–west pattern in the vicinity of the equator, that is, a tilt to the thermocline. The time series indicates that it consists of an ENSO-related signal and a trend. The relaxation of the east–west slope of the thermocline, associated with warm (ENSO) episodes, is greater for the model with data assimilation (RA2). The trend is such that, with data assimilation, the east–west slope of the thermocline tended to be greater (less) in the earlier (later) part of this period; that is, the thermocline in the eastern tropical Pacific appears to be deeper during the late 1980s to early 1990s than during the early 1980s. Observed SST and low-level (850 hPa) atmospheric winds (not shown) show a generally weaker easterly trade wind and warmer SST in the tropical Pacific during the recent period since 1990 than during the early 1980s, suggesting evidence of interdecadal climate variability. (This suggests that an anomaly coupled model that uses a single prescribed stress climatology over

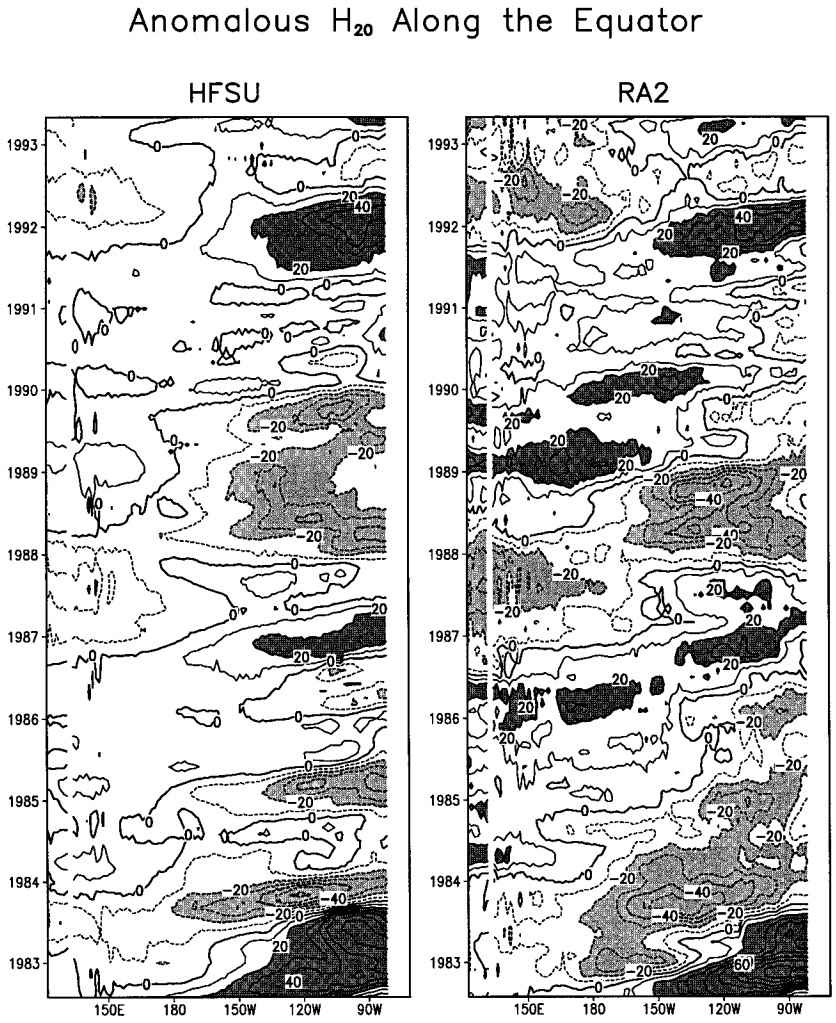

FIG. 1. Anomalous depth of the 20°C isotherms along the equator for the HFSU (left) and RA2 (right) ocean initial conditions. The contour interval is 10 m. Anomalies greater (less) than 20 m (−20 m) are indicated by dark (light) shading.

the whole period may not be the best approach for forecasting climate variability for the entire period.)

The second EOF, in the near equatorial region, has its largest amplitude in the central-western Pacific. The time series indicates that with data assimilation the thermocline is deeper in this location before warm episodes and shallower before cold episodes. The thermocline variability in the equatorial Pacific is related to that of upper-ocean heat content and is important to ENSO evolution (Wyrtki 1985; Latif and Graham 1992; Latif et al. 1993). Thus, accurate initialization of thermocline variability in the central equatorial Pacific should also have a significant impact on forecast skill. The indications from the spatial structure and temporal evolution of the second EOF is that with assimilation the ocean is more accurately ''initialized'' for later occurrence.

To understand the impact of these thermocline depth differences on forecast skill, we examined four individual cases from the F-RA2 and the F-HFSU forecasts. Forecasts for the northern winters (December–February) of 1988–89 and 1991–92 are shown in Fig. 3. The former period coincides with a strong cold episode and the latter coincides with a warm episode. The approximate initial times of these two forecasts are indicated by asterisks in the lower panel of Fig. 2. Both forecasts were initiated during the northern summer (June–August), starting on the first of each month. Each example shown here is an average of three individual forecasts. The average lead time for these examples is two seasons. Comparison of the observed and forecast SST anomalies for both periods indicates that forecasts initiated from the RA2 and the FSU initial conditions were able to capture the pattern of strong SST anomalies regardless of the thermocline depth differences in these ocean initial conditions. The amplitude of the SST anomalies appears to be a little better in the F-RA2 forecasts.

Forecasts for September–November (SON) 1986 and for December 1989–February 1990 (DJF) are shown in

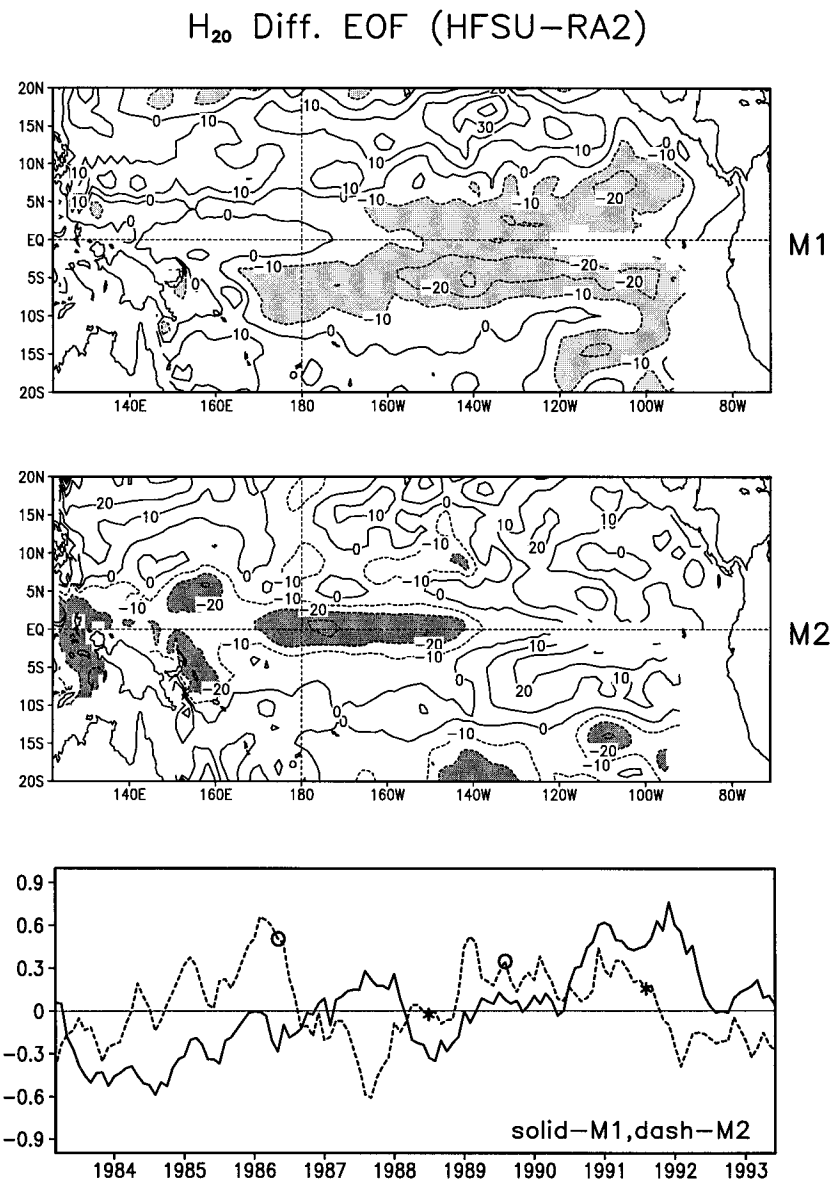

FIG. 2. The first (top) and second (middle) EOFs for the monthly mean difference of 20°C isotherms between HFSU and RA2 ocean initial conditions. These two EOFs account for 9% and 8.5% of total variance, respectively. Time series for the first EOF (solid) and the second EOF (dash) are shown in the lower panel. The asterisks and circles in the lower panel indicate the approximate initial times for forecast examples shown in Fig. 3 and Fig. 4 (see section 4).

Fig. 4. The SON forecast is the average of two individual forecasts starting on 1 May and 1 June 1986; the DJF forecast is the average of three forecasts initiated on 1 June, 1 July, and 1 August 1989. The approximate initial times of these two forecasts are indicated by circles in the lower panel of Fig. 2. Both examples show F-RA2 forecasts are closer to observations than F-HFSU forecasts. Particularly, the F-HFSU forecasts for the DJF 1989–90 were predicting a mild cold episode that did not occur. Examination of the dashed curve in the bottom panel in Fig. 2, as indicated by the asterisks and circles, showed that in terms of the second EOF the difference between the HFSU and RA2 ocean initial conditions for the reasonably good forecasts for the major episodes (Fig. 3) was less than for the poorer forecasts shown in Fig. 4. Since RA2 closely follows the observations, large differences from it can be expected to lead to poorer forecasts, as in fact was the case. In both poor forecasts (Fig. 4), the F-HFSU predicted colder equatorial SSTs than were observed. This was also the case of the HFSU initial conditions (shallower thermocline depth than RA2 in the central equatorial Pacific) as indicated by the second EOF pattern shown in Fig. 2.

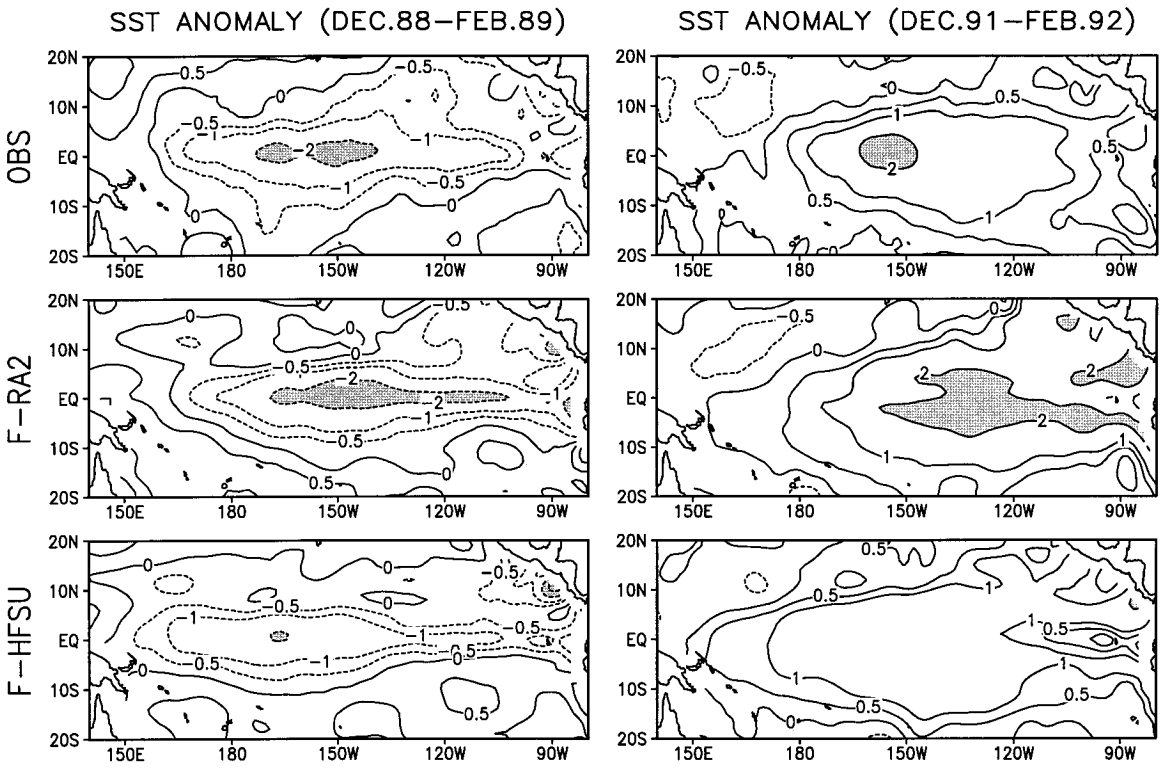

FIG. 3. Observed and forecast SST anomalies for winter (December–February) of 1988/89 (left panels) and 1991/92 (right panels). Observed SST anomalies are shown in the top panels; forecast SST anomalies from F-RA2 are shown in the middle panels. Forecast SST anomalies from F-HFSU are shown in the lower panels. Light (dark) shading indicates SST anomalies above 1°C (2°C) or below −1°C (−2°C). Contour interval is 1°C. In addition, contours of 0.5°C and −0.5°C are shown.

These comparisons suggest that for strong cold or warm episodes, the forecasts give good indications of developing tropical Pacific SST anomaly patterns. This occurs regardless of whether or not the ocean initial conditions are produced with assimilation of subsurface temperature data, provided that a good quality wind stress forcing field that can capture strong low-frequency basin-scale variability is available. However, when the strong low-frequency basin-scale signals are absent, errors in wind stress forcing and in the ocean model sometimes could be sufficiently large to produce false signals in the ocean initial conditions and have led to poor forecasts. A summary of the results of all these experiments is given in the following discussion.

Anomaly correlation coefficients (ACC) and root mean square (rms) errors as a function of forecast lead times for area-averaged SST anomalies between the two sets of forecasts (F-RA2 and F-HFSU) and the observations are shown in Fig. 5a. Recall that F-RA2 used initial conditions obtained with data assimilation, while F-HFSU did not. The index area is a region in the eastern-central equatorial Pacific (5°S–5°N, 170°–120°W). We refer to this area as the SST-3 region. In the left panel, ACC for area-averaged SST anomalies between the F-RA2 and the observations (solid) and between the F-HFSU and the observations (dot–dashed) are depicted. These ACCs for both experiments are based on 1-yr forecasts initiated monthly from October 1983 to October 1993. However, only forecasts starting in May through November during this period are shown in Fig. 5a. The forecasts are verified against area-averaged SST anomalies derived from the monthly mean SST analyses of Reynolds and Marsico (1993). The results clearly indicate that, given the same CGCM, forecasts that used ocean initial conditions produced with data assimilation outperform forecasts that used ocean initial conditions produced without data assimilation.

The solid and dot–dashed curves in Fig. 5b are similar to those in Fig. 5a except forecasts are initiated during the northern winter season (December–February) for 1983/84 to 1992/93. A total of 30 1-yr forecasts are verified against observations. Surprisingly, the skills for F-RA2 (solid) and F-HFSU (dot–dashed) indicate a reversal of the results presented in Fig. 5a. This suggests that, for the CMP6 model, data assimilation made the forecasts starting in the winter seasons worse. The Ji et al. (1994) paper showed that the skill of NCEP forecasts starting in the winter season is significantly lower than those starting in other seasons. They attributed this to the so-called spring prediction barrier (Zebiak and Cane

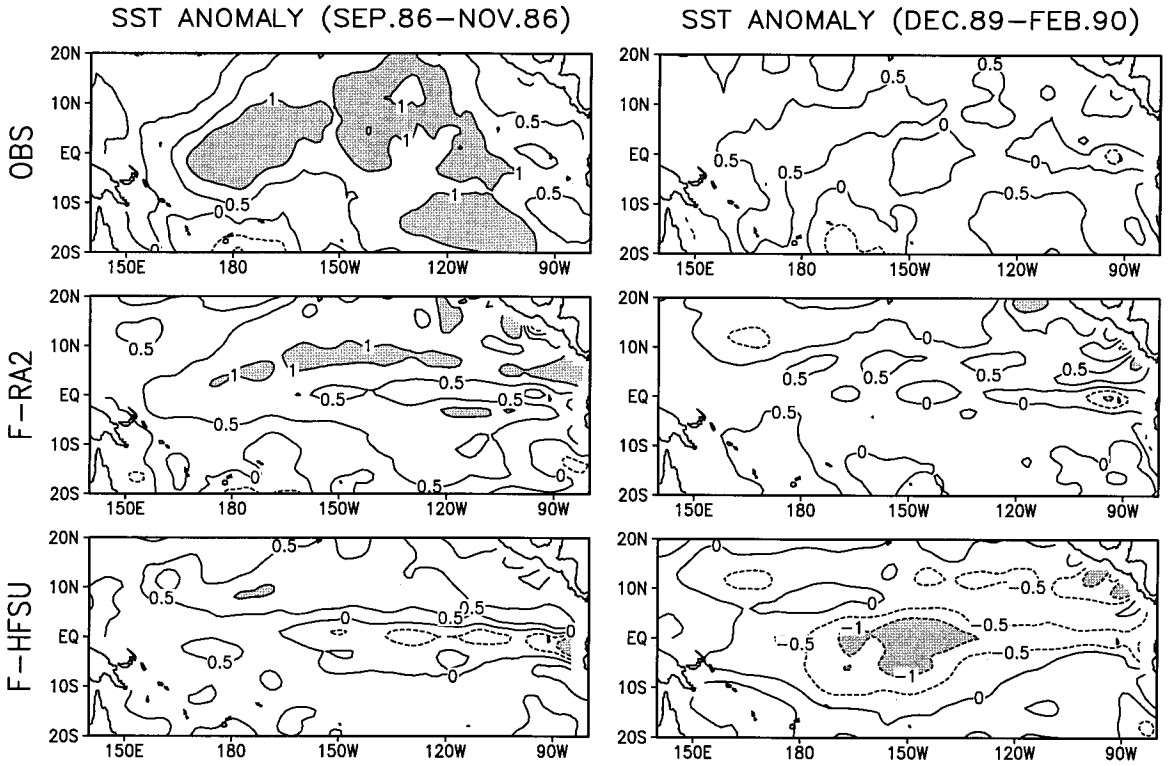

FIG. 4. Same as in Fig. 3 but for September–November 1986 (left) and December 1989–February 1990 (right). Light (dark) shading indicates SST anomalies above 0.5°C (1°C) or below −0.5°C (−1°C). Contour interval is 0.5°C.

1987; Blumenthal 1991). Although northern spring in general has proven to be a difficult season to forecast, the F-HFSU experiment shown here indicates that the low skill for those winter forecasts using the CMP6 model are to a great extent the result of errors in the forecast system.

The reasons why data assimilation had a detrimental effect on forecasts initiated in the winter season for the CMP6 model are unclear. There are indications that model errors and imbalances resulting from difference in the mean states between oceanic initial conditions and the forecast model may play a significant role. Results from forecast experiments using a later version of the NCEP coupled model and a more recent set of ocean analyses (dashed curves in Fig. 5b) indicate that the skill for these forecasts initiated in winter is comparable to that of the F-HFSU. This later version of the NCEP coupled model is similar to the CMP6 model, but it includes a statistical correction procedure to correct stress anomalies produced from the AGCM before they are used to force the ocean during coupled forecasts (Ji and Leetmaa 1994). The dashed curve in Fig. 5b as compared to the solid curve in Fig. 5a suggests that northern winter is a more difficult season for initialization of coupled forecast models than for summer/fall, at least for the NCEP coupled models. Obtaining the ''best'' oceanic initial conditions for the winter season, in any case, appears to be more challenging than other times during the year.

The combined skill for all seasons using the CMP6 model unambiguously indicates overall improvement in forecast skill (Fig. 6). However, these results suggest that initialization using data assimilation as implemented for the coupled models at NCEP did not provide answers to all the problems associated with improving initialization for climate forecasts. Other limiting factors in the climate forecast system such as the quality of the wind forcing, model errors, and properly balancing the coupled system during initialization for the proper scale of variability are just as significant. Without addressing those issues, data assimilation only improves forecast skill to a certain limit.

5. The impact of the TOGA–TAO temperature data

Currently, data from the TOGA–TAO buoys provides basinwide, continuous coverage of the equatorial Pacific. Real time data from the TAO buoys first became available in the late 1980s, and the amount of the TAO data has increased steadily since the early 1990s. Presently, there are more than 65 moored buoys deployed in the tropical Pacific. The TAO array extends meridionally to 8°S and 8°N.

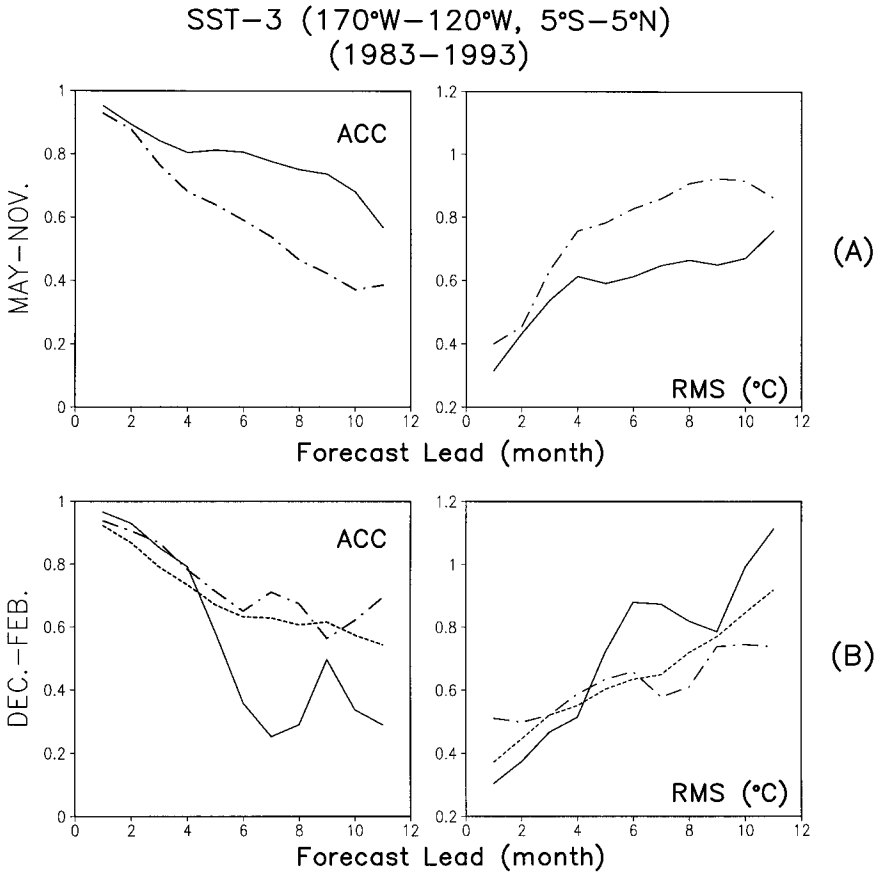

FIG. 5. (a) Anomaly correlation coefficients (ACC, left) and rms errors (right) between forecasts and observations for area-averaged SST anomalies in the SST-3 region (5°S–5°N, 170°–120°W). Solid (dash–dotted) curves are for F-RA2 (F-HFSU) forecasts. Skill was computed based on forecasts starting monthly on 1 May through 1 November for the period of October 1983–October 1993. (b) Solid and dash–dotted curves are similar to those in (a), except that the ACC and rms errors are for forecasts initiated during northern winter months (December–February) for 1983/84 to 1992/93. Dashed curves are ACC and rms errors for forecasts of northern winter starts for the same period but using a later version of the NCEP coupled model.

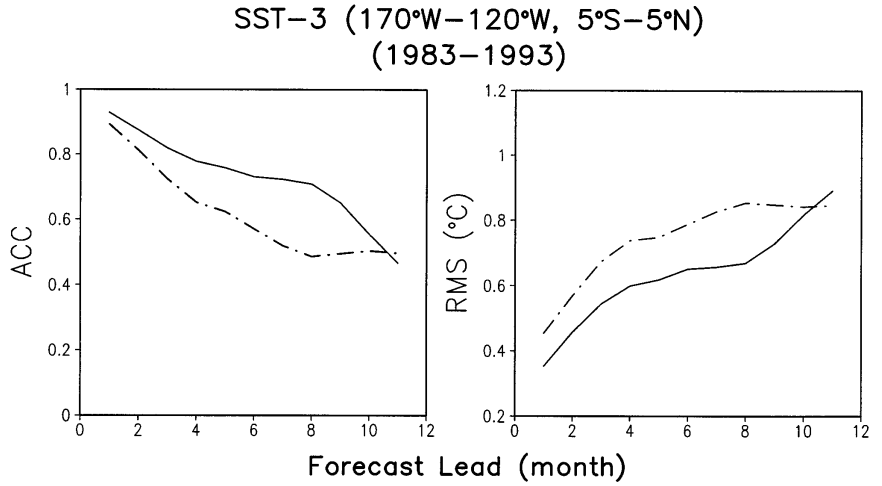

FIG. 6. Same as in Fig. 5a, except that the ACC and rms errors are based on all forecasts using CMP6 model regardless of their starting month.

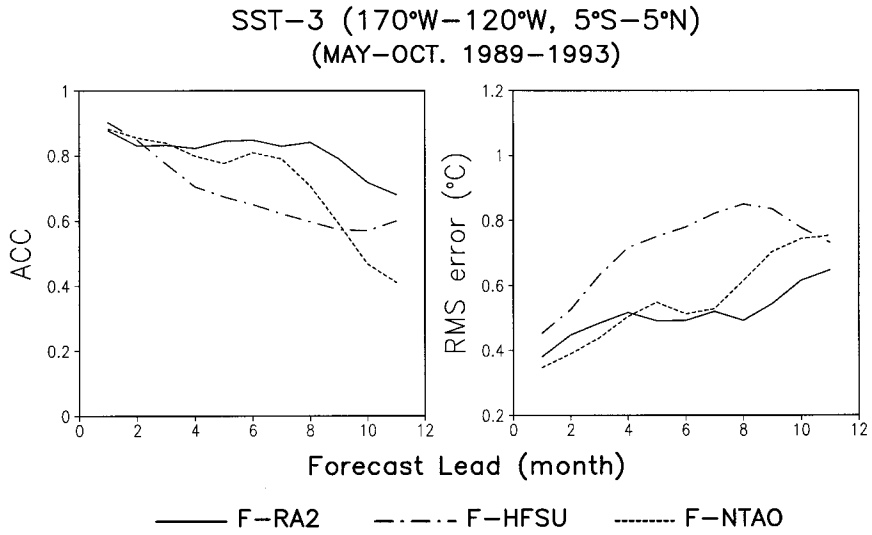

FIG. 7. Anomaly correlation coefficients (ACC, left) and rms errors (right) between forecasts and observations for area-averaged SST anomalies in the SST-3 region (5°S–5°N, 170°–120°W). Solid curves are for F-RA2 forecasts, dashed curves are for F-NTAO forecasts, and dot–dashed curves are for F-HFSU forecasts (see section 3). All ACCs were computed based on 30 forecasts starting monthly on 1 May through 1 October for the period of 1989–93.

Skill comparisons for F-RA2, F-NTAO, and F-HFSU forecasts are shown in Fig. 7. Recall that the F-RA2 used the ocean initial conditions produced by assimilation of all upper-ocean temperature data, while the F-NTAO used the ocean initial conditions that assimilated XBT but not TAO data. Each curve is based on 30 cases of 1-yr forecasts initiated monthly on 1 May–1 October for 1989–93. This period was chosen because significant amounts of TAO data were not available prior to early 1989.

Comparison of the skill of these three sets of forecasts suggests that improvement in skill is gained by assimilation of upper-ocean temperature data from the TOGA–TAO buoys into the ocean initial conditions. The improvement is most pronounced for forecasts of lead times longer than two to three seasons. Caution needs to be exercised in the conclusions to be drawn from these comparisons. The positive impact of TAO data on forecast skill is obviously significant; however, the primary reason for the positive impact of the TAO data probably results from its contribution to improving the spatial and temporal coverage of subsurface observations. The spatial distribution of subsurface temperature data in the tropical Pacific collected during October 1993 is shown in Fig. 8. It is obvious that large areas in the eastern and western tropical Pacific are covered primarily by the TAO buoys. Furthermore, each moored buoy reports subsurface temperature profiles daily, while each dot in the figure represents a single XBT observation. Without TAO, the data quantity would be significantly less; in fact, TAO contributes more than 50% of the total observations in the tropical Pacific.

6. Summary

In this paper, we evaluated the forecast skill of the National Centers for Environmental Prediction coupled

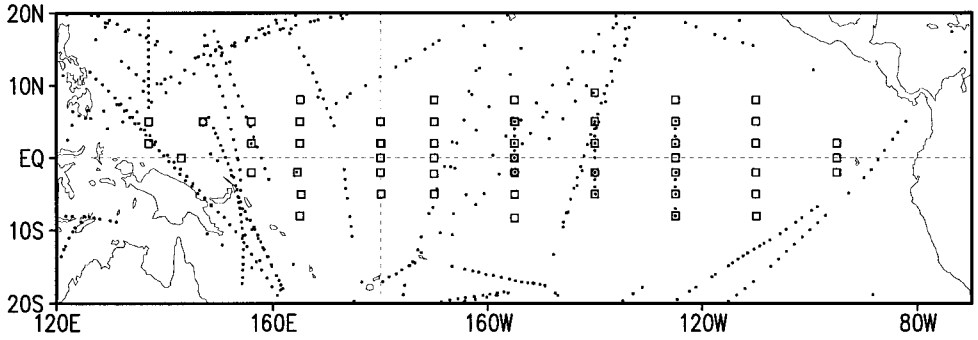

FIG. 8. Distribution of subsurface temperature observations in the tropical Pacific for October 1993. Open squares represent TOGA–TAO buoy locations, daily temperature profiles are available from these buoy sites; dots represent single XBT observations.

model. The forecasts were initiated from various ocean initial conditions. These were produced with and without assimilation of upper ocean temperature data, and with data assimilation but without including the TOGA–TAO buoy data. Comparisons of forecast skills for these various sets of forecast experiments indicate the following.

1) Assimilation of observed upper ocean temperature data into an ocean model can significantly improve the forecast skill of a coupled GCM. This is because assimilation of subsurface temperature data compensates for errors in wind fields and inadequate physical parameterizations in ocean models.
2) Although analyses produced with data assimilation describe the states of the ocean more accurately than those produced with wind forcing alone, errors in coupled models and imbalance in the mean states between the analyses and conditions in the coupled model limit forecast skill for forecasts initiated in the winter season and at longer lead times. Further improvements in forecast skill must take into consideration factors such as what features of the variability most impact forecast skill and hence need accurate initialization and improvements in the coupled forecast model itself. Data assimilation by itself cannot address all these issues.
3) TAO array provides much improved spatial and temporal data coverage in the tropical Pacific, which is the key region for ENSO development. Inclusion of subsurface temperature data from the TAO buoys together with basinwide XBT data to initialize ocean fields resulted in a significant increase in forecast skill for the NCEP coupled model.

Acknowledgments. Support for this research is provided by NOAA's Office of Global Program through the Climate and Global Change Program.

REFERENCES

Barnett, T. P., M. Latif, N. E. Graham, M. Flügel, S. Pazan, and W. White, 1993: ENSO and ENSO related predictability. Part I: Prediction of equatorial Pacific sea surface temperatures with a hybrid coupled ocean–atmosphere model. *J. Climate,* **6,** 1545–1566.

Bjerknes, J., 1969: Atmospheric teleconnections from the equatorial Pacific. *Mon. Wea. Rev.,* **97,** 163–172.

Blumenthal, M. B., 1991: Predictability of a coupled ocean–atmosphere model. *J. Climate,* **4,** 766–784.

Bryan, K., 1969: A numerical method for the study of the World Ocean. *J. Comput. Phys.,* **4,** 347–376.

Cane, M. A., S. E. Zebiak, and S. C. Dolan, 1986: Experimental forecasts of El Nino. *Nature,* **321,** 827–832.

Chen, D., S. E. Zebiak, A. J. Busalacchi, and M. A. Cane, 1995: An improved procedure for El Nino forecasting. *Science,* **269,** 1699–1702.

Cox, M. D., 1984: A primitive, 3-dimensional model of the ocean. GFDL Ocean Group Tech. Rep. No. 1, Geophysical Fluid Dynamics Laboratory, 143 pp. [Available from Geophysical Fluid Dynamics Laboratory/NOAA, Princeton University, Princeton, NJ 08540.]

Derber, J., and A. Rosati, 1989: A global oceanic data assimilation system. *J. Phys. Oceanogr.,* **19,** 1333–1347.

Goldenberg, S. B., and J. J. O'Brien, 1981: Time and space variability of tropical Pacific wind stress. *Mon. Wea. Rev.,* **109,** 1190–1207.

Halpern, D., and M. Ji, 1993: An evaluation of the National Meteorological Center weekly hindcast of upper-ocean temperature along the eastern Pacific equator in January 1992. *J. Climate,* **6,** 1221–1226.

Hao, Z., and M. Ghil, 1994: Data assimilation in a simple tropical ocean model with wind stress errors. *J. Phys. Oceanogr.,* **24,** 2111–2128.

Harrison, D. E., 1989: On climatological mean wind stress and wind stress curl fields over the world ocean. *J. Climate,* **2,** 57–70.

Hayes, S. P., L. J. Mangum, J. Picaut, A. Sumi, and K. Takeuchi, 1991: TOGA–TAO: A moored array for real-time measurements in the tropical Pacific Ocean. *Bull. Amer. Meteor. Soc.,* **72,** 339–347.

Hellerman, S., and M. Rosenstein, 1983: Normal monthly wind stress over the world ocean with error estimates. *J. Phys. Oceanogr.,* **13,** 1093–1104.

Horel, J. D., and J. M. Wallace, 1981: Planetary scale atmospheric phenomena associated with the Southern Oscillation. *Mon. Wea. Rev.,* **109,** 813–829.

Ji, M., and A. Leetmaa, 1994: An improved coupled ocean–atmosphere model for ENSO predictions. *Proc. 19th Climate Diagnostics Workshop,* College Park, MD, NOAA, 88–91.

——, and T. M. Smith, 1995: Ocean model responses to temperature data assimilation and varying surface wind stress: Intercomparisons and implications for climate forecast. *Mon. Wea. Rev.,* **123,** 1811–1821.

——, A. Kumar, and A. Leetmaa, 1994: An experimental coupled forecast system at the National Meteorological Center: Some early results. *Tellus,* **46A,** 398–418.

——, A. Leetmaa, and J. Derber, 1995: An ocean analysis system for seasonal to interannual climate studies. *Mon. Wea. Rev.,* **123,** 460–481.

Kleeman, R., A. M. Moore, and N. R. Smith, 1995: Assimilation of subsurface thermal data into an intermediate tropical coupled ocean–atmosphere model. *Mon. Wea. Rev.,* **123,** 3103–3113.

Kumar, A., M. P. Hoerling, M. Ji, A. Leetmaa, and P. Sardeshmukh, 1996: Assessing a GCM's suitability for making seasonal predictions. *J. Climate,* **9,** 115–129.

Latif, M., and M. Flügel, 1991: An investigation of short-range climate predictability in the tropical Pacific. *J. Geophys. Res.,* **96** (C2), 2661–2673.

——, and N. E. Graham, 1992: How much predictive skill is contained in the thermal structure of an OGCM? *J. Phys. Oceanogr.,* **22,** 951–962.

——, A. Sterl, E. Maier-Reimer, and M. M. Junge, 1993: Structure and predictability of the El Nino/Southern Oscillation phenomenon in a coupled ocean–atmosphere general circulation model. *J. Climate,* **6,** 700–708.

——, T. P. Barnett, M. A. Cane, M. Flügel, N. E. Graham, H. von Storch, J. S. Xu, and S. E. Zebiak, 1994: A review of ENSO prediction studies. *Climate Dyn.,* **9,** 167–179.

McPhaden, M. J., 1993: TOGA-TAO and the 1991–93 El Nino–Southern Oscillation event. *Oceanography,* **6,** No. 2, 36–44.

Mo, K. C., M. Ji, and A. Leetmaa, 1994: Forecast errors in the NMC coupled ocean–atmosphere model. *Proc. 19th Climate Diagnostic Workshop,* College Park, MA, NOAA, 393–395.

Neelin, J. D., M. Latif, and F.-F. Jin, 1994: Dynamics of coupled ocean–atmosphere models: The tropical problem. *Annu. Rev. Fluid Mech.,* **26,** 617–659.

Oberhuber, J. M., 1988: An atlas based on the ''COADS'' data set: The budgets of heat, buoyancy and turbulent kinetic energy at the surface of the global ocean. Rep. 15, 20 pp. [Available from Max-Planck-Institut Fur Meteorologie, Bundesstrasse 55, Hamburg, Germany.]

Philander, S. G. H., W. J. Hurlin, and A. D. Seigel, 1987: A model of the seasonal cycle in the tropical Pacific Ocean. *J. Phys. Oceanogr.,* **17,** 1986–2002.

Rasmusson, E. M., and J. M. Wallace, 1983: Meteorological aspects of the El Nino/Southern Oscillation. *Science,* **222,** 1195–1202.

Reed, R. K., 1977: On estimating insolation over the ocean. *J. Phys. Oceanogr.,* **7,** 482–485.

Reynolds, R. W., and D. C. Marsico, 1993: An improved real-time global sea surface temperature analysis. *J. Climate,* **6,** 114–119.

——, K. Arpe, C. Gorden, S. P. Hayes, A. Leetmaa, and M. J. McPhaden, 1989: A comparison of tropical Pacific surface wind analysis. *J. Climate,* **2,** 105–111.

Ropelewski, C. F., and M. S. Halpert, 1986: North American precipitation and temperature patterns associated with the El Nino/Southern Oscillation (ENSO). *Mon. Wea. Rev.,* **114,** 2352–2362.

——, and ——, 1987: Global and regional scale precipitation patterns associated with the El Nino/Southern Oscillation. *Mon. Wea. Rev.,* **115,** 1606–1626.

Rosati, A., K. Miyakoda, and R. Gudgel, 1997: The impact of ocean initial conditions on ENSO forecasting with a coupled model. *Mon. Wea. Rev.,* **125,** 754–772.

Wyrtki, K., 1975: El Nino—The dynamical response of the equatorial Pacific to atmospheric forcing. *J. Phys. Oceanogr.,* **5,** 572–584.

——, 1985: Water displacements in the Pacific and the genesis of El Nino cycles. *J. Geophys. Res.*, **90** (C4), 7129–7132.

Zebiak, S. E., and M. A. Cane, 1987: A model El Nino–Southern Oscillation. *Mon. Wea. Rev.,* **115,** 2262–2278.